

Contents

Step 1: Corneal Imaging

Chapter 1	Topography and Tomography Science	3
	<i>Main Tomographic Maps and Profiles</i>	3
	<i>Topographic and Tomographic Features in Ectatic Corneal Disorders</i>	42
Chapter 2	Wavefront Science	51
	<i>Principles of Wavefront and Wavefront Analysis</i>	51
	<i>Types of Aberrations</i>	53
	<i>Measurement of Aberrations</i>	61
	<i>Wavefront Maps</i>	71
	<i>Changes of Aberrations with Age</i>	75
	<i>Wavefront in FFKC Detection</i>	77
Chapter 3	Optical Coherence Tomography (OCT)	79
	<i>Introduction</i>	79
	<i>Normal Anterior Eye</i>	79
	<i>Clinical Application of Anterior OCT</i>	80
Chapter 4	Corneal Biomechanics	100
	<i>Introduction</i>	100
	<i>Clinical Impact of Corneal Biomechanics</i>	101
	<i>Measuring Corneal Biomechanics</i>	106

Step 2: Main Refractive Options

Chapter 5	Main Refractive Options	117
	<i>Photo Refractive Treatment (PRT)</i>	117
	<i>Surface Ablation Combined with Corneal Collagen Cross Linking</i>	152
	<i>Phakic IOL (PIOL)</i>	154
	<i>Refractive Lens Exchange (RLE)</i>	156

Step 3: Rules and Guidelines in Refractive Surgery

Chapter 6 Rules and Guidelines in Refractive Surgery 173

Thickness Rules 173

K-reading Rules 179

Disparity between Topographic Astigmatism (TA) and Manifest Astigmatism (MA) 183

Suboptimal Correction Rule 191

Pupil Center and Angle Kappa Rule 191

Pupil Diameter Considerations 192

Cyclotorsion 193

Amblyopia 194

Enhancement Concepts 195

Step 4: Start Off

Chapter 7 Clinical Approach 201

Psychosocial Approach 201

Medical Approach 202

Examination 212

Chapter 8 Avoidable Refractive Surgery Complications 221

Complications Related to PRT 221

Complications Related to PIOL 241

Complications in Refractive Lens Exchange 243

Step 5: Case Study

Chapter 9 Case Study 255

Introduction 255

Reading and Interpreting Corneal Tomography 255

Reading and Interpreting Wavefront 256

Case No. 1 257

Case No. 2 265

Case No. 3 273

Case No. 4 281

Case No. 5 297

Case No. 6 306

Case No. 7 319

Case No. 8 332

Case No. 9 347

Index

361

Optical Coherence Tomography (OCT)

INTRODUCTION

CORE MESSAGE

- Optical coherence tomography (OCT) is an important complementary investigation
- It gives optical images with higher resolution than Scheimpflug-based devices
- It measures corneal thickness and gives a pachymetry map that is less affected by corneal opacities
- It can be used in diagnosis and treatment of refractive complications and some corneal pathologies
- It is taking an important role in detecting early KC and other ectatic corneal disorders
- It is taking an important role in diagnosing and planning for management of glaucoma

Optical coherence tomography (OCT) is a fundamentally new type of medical diagnostic imaging technology that performs high-resolution, micron-scale, cross-sectional imaging of the internal microstructure in biological tissues by measuring the intensity and echo time delay of light.

OCT is a powerful imaging modality because it enables the real-time, *in situ* imaging of tissue structure or pathology with resolutions of 1 to 15 μm , which is one to two orders of magnitude finer than conventional clinical imaging technologies such as ultrasound, magnetic resonance imaging (MRI), or computed tomography (CT). The operation of OCT is analogous to ultrasound B-mode imaging or radar except that light is used rather than acoustic or radio waves. OCT is especially suited for diagnostic applications in ophthalmology because of the ease of optical access to the anterior and posterior eye. The physical basis of imaging depends on the contrast in optical reflectivity between different tissue microstructures.

NORMAL ANTERIOR EYE

Anterior Chamber

Figure 3.1 displays an OCT image of a normal anterior chamber obtained from a healthy human eye. Clearly identifiable structures include the cornea, sclera, iris and lens anterior capsule. The strongest reflected signals arise from the epithelial surface of the cornea and the highly scattering sclera and iris. Smaller amounts of backscatter are visible from within the nominally transparent cornea and lens. The backscatter intensity gradually decreases from central to peripheral cornea. This signal fading may be attributed to highly angle-dependent backscattering from the stromal collagen lamellae, which run parallel to the corneal surface. The limbus appears as the angled interface between the cornea and the sclera. The normal “watch glass” insertion of the cornea into the sclera is clearly visible.

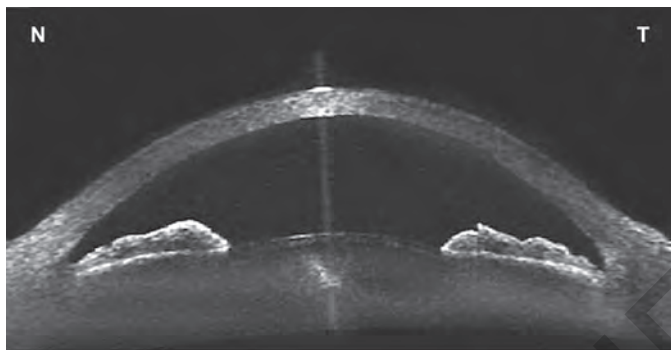


Fig. 3.1 OCT view of anterior chamber obtained from a normal healthy eye.

Cornea and Angle

By narrowing the field-of-view, OCT can be used to obtain high resolution images of corneal microstructure. A magnified OCT image of the cornea appears in **Figure 3.2**, which differentiates the corneal epithelium, Bowman's layer, stroma, Descemet's membrane and endothelium based on the differences in their optical properties. Normal corneal thickness is 550 μ m in average (450 – 700 μ m) and consists of the followings: 30–80 μ m for epithelium, 16 μ m for Bowman, 380–480 μ m for stroma, and 20 μ m for Descemet and endothelium. A close-up view of the angle region (**Fig. 3.3**) shows the iris contour and epithelium, the corneoscleral limbus and the ACA. Structures in the angle region such as the trabecular meshwork and canal of Schlemm are not clearly visualized in the tomogram since the incident and backscattered light is highly attenuated after traversing the overlying scleral tissue.

Pachymetry Map

Anterior OCT measures corneal thickness and displays a pachymetry map provided with indices that help in detection of KC and ectatic corneal disorders (**Fig. 3.4**).

CLINICAL APPLICATION OF ANTERIOR OCT

Anterior OCT is used for diagnosis and planning and guiding treatment.

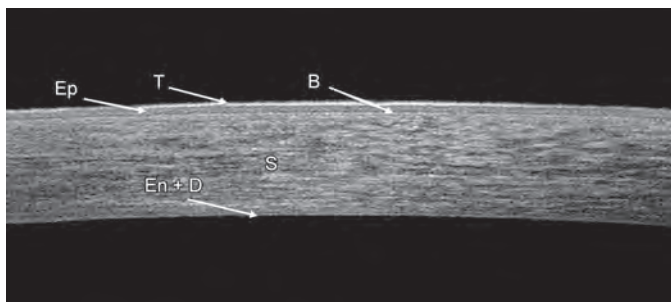


Fig. 3.2 Corneal layers by OCT. T: tear; Ep: epithelium; B: Bowman; S: stromal; En: endothelium; D: Descemet.

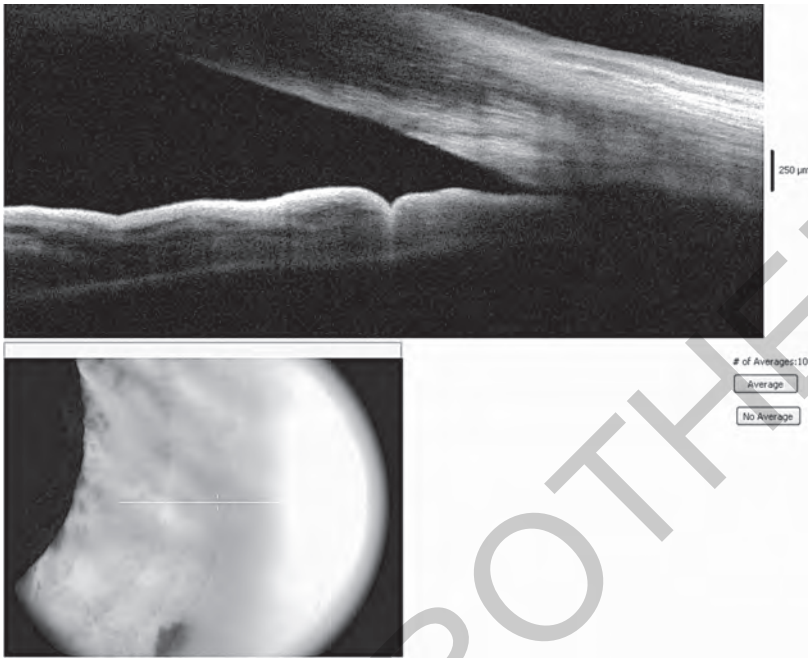


Fig. 3.3 OCT view of anterior chamber angle.

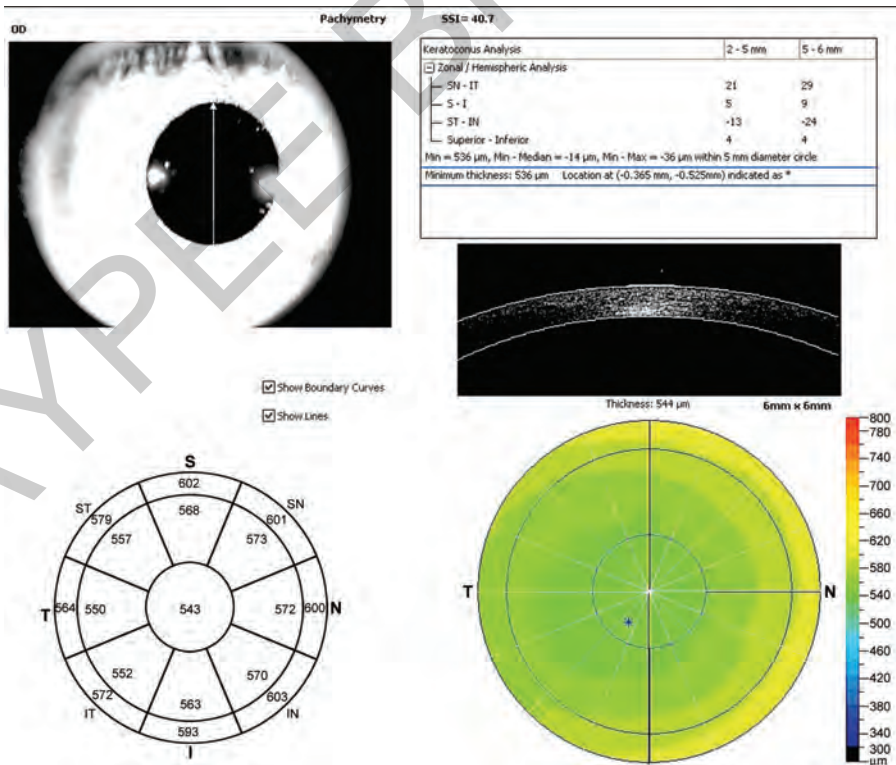


Fig. 3.4 OCT pachymetry map. In the upper right is KC detection indices.

Diagnosis

Anterior OCT is used to aid diagnosis of several pathologies, but we are concerned here in what is related to refractive surgery.

Corneal Lesions

1. Sub Bowman Calcifications (SBCs):

Case 1: A 32 y/o female.

Figure 3.5 is her Pentacam tomography showing irregular cornea.

Figure 3.6 is corneal tomogram 3D image showing corneal calcifications.

Figure 3.7 is anterior OCT showing the location and depth of the calcifications.

N.B.: **Figures 3.5 to 3.7** are registered under author's name in "Atlas of Ophthalmology: Online Multimedia Database."

Case 2: 14 y/o male that has bilateral SBCs. His twin brother has the same disease.

Figure 3.8 is anterior OCT of the right eye showing the location and depth of the calcifications.

Figure 3.9 is the OCT pachymetry map showing irregular thickness.

Figure 3.10 is the same eye after treatment with photo therapeutic keratectomy (PTK).

Figure 3.11 is the OCT pachymetry map post-PTK; notice the regular pattern.

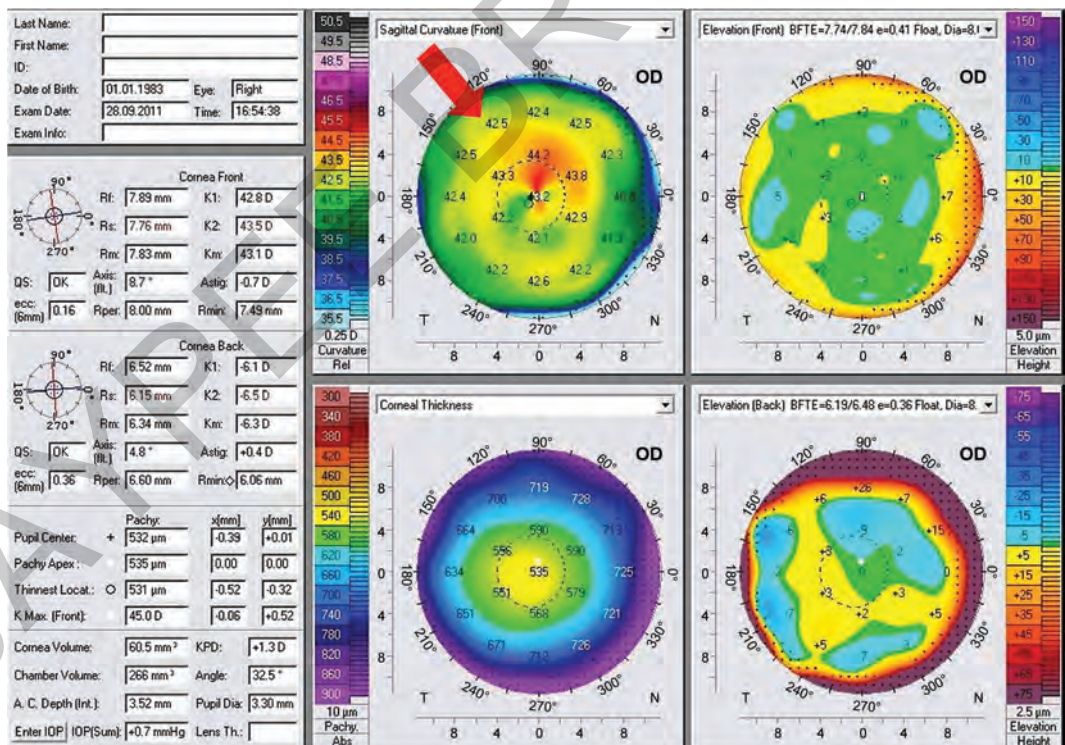


Fig. 3.5 Sun Bowman Calcifications (SBCs). Corneal tomography; notice the AB/SS pattern (red arrow).

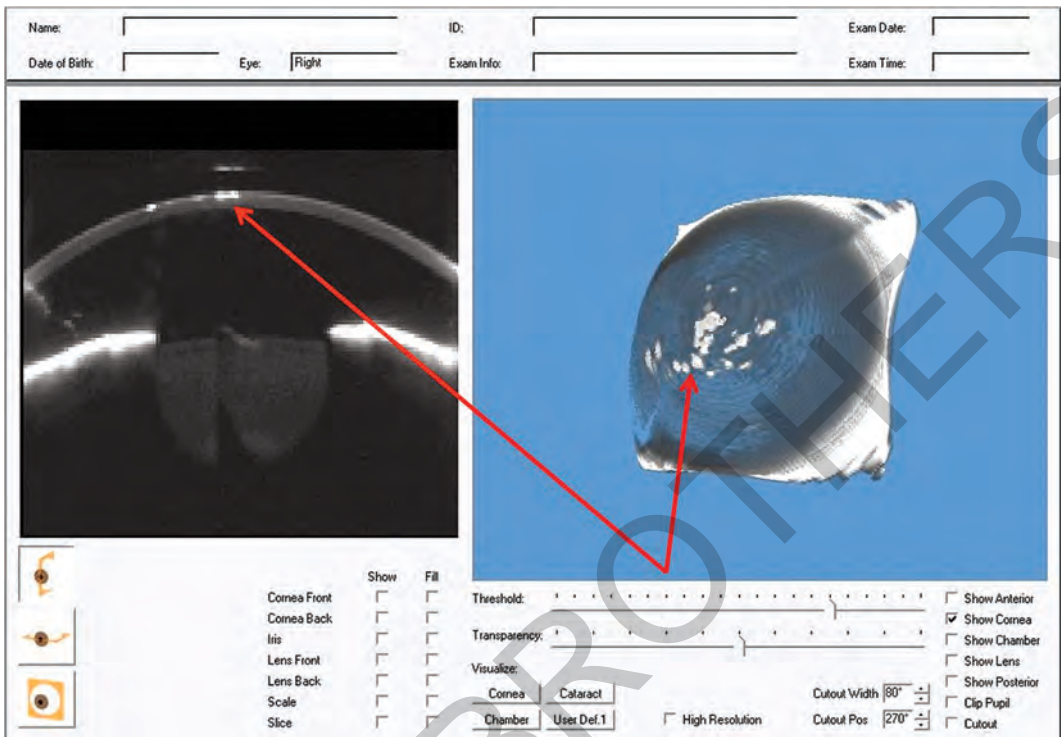


Fig. 3.6 SBCs. Scheimpflug tomogram; red arrows point at the calcifications.

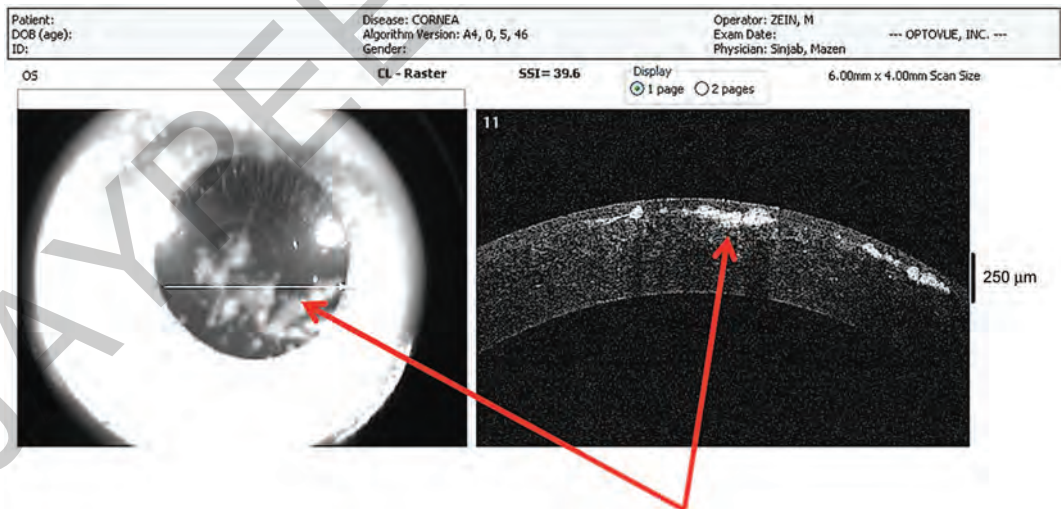


Fig. 3.7 SBCs. OCT view; red arrows point at the calcifications. Thickness and depth of the calcifications can be measured by OCT.

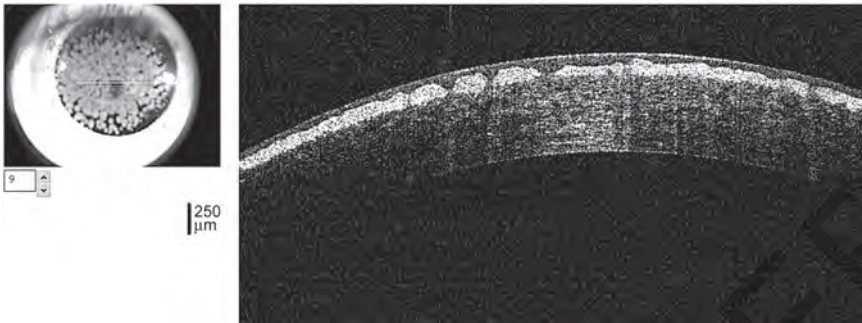


Fig. 3.8 SBCs. OCT view of a cornea with a severe bilateral disease in a twin of males.

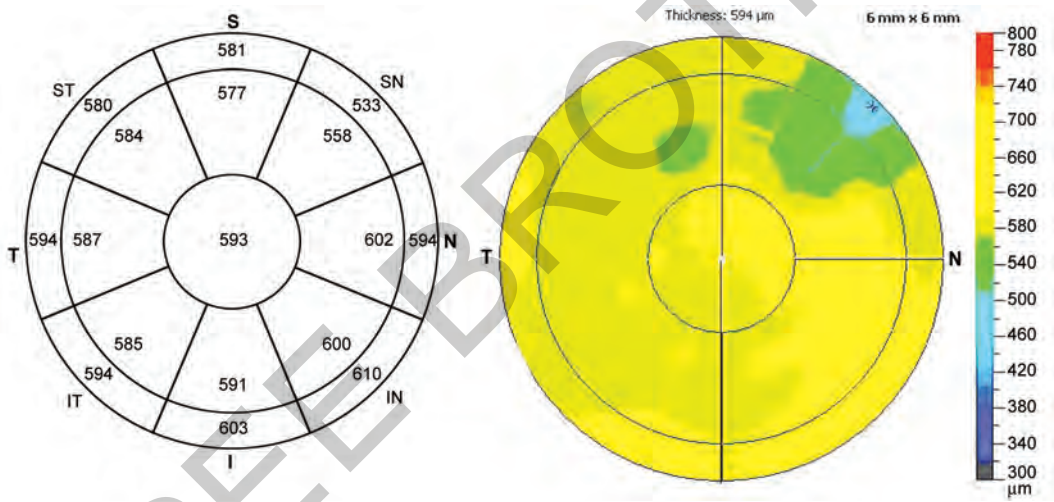


Fig. 3.9 SBCs. OCT pachymetry map; irregular thickness.



Fig. 3.10 SBCs. OCT view after PTK treatment.

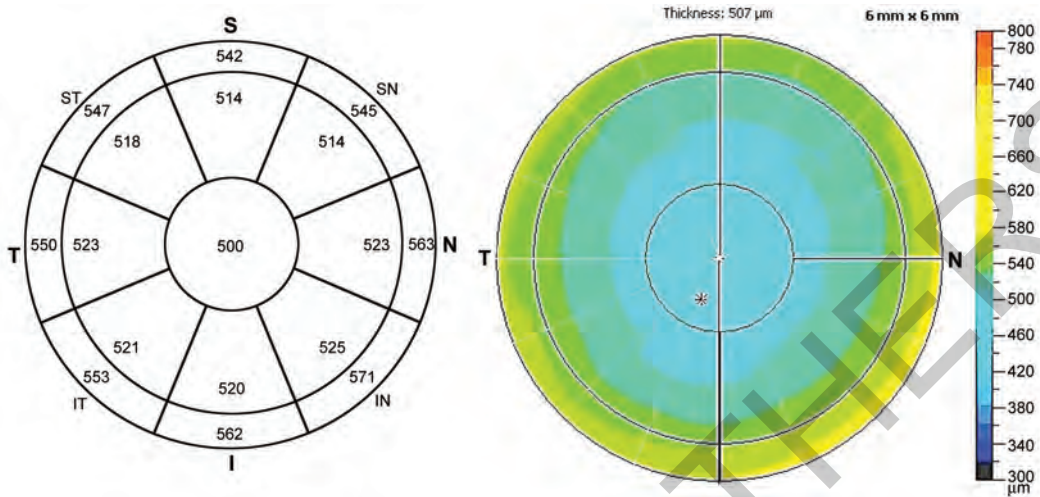


Fig. 3.11 SBCs. OCT pachymetry map after PTK treatment; regular thickness.

2. Salzmann's Nodular Degeneration (SND):

Salzmann's nodular degeneration (SND) is a lesion located above Bowman layer as shown in **Figures 3.12 and 3.13**. **Figure 3.14** is the OCT pachymetry map showing the thickened part of the cornea, corresponding to the nodule (red arrow).

3. Posterior corneal abnormality:

Posterior corneal abnormality includes Descemet folds (**Fig. 3.15**), cornea guttata and Fuch's endothelial dystrophy (**Fig. 3.16**).

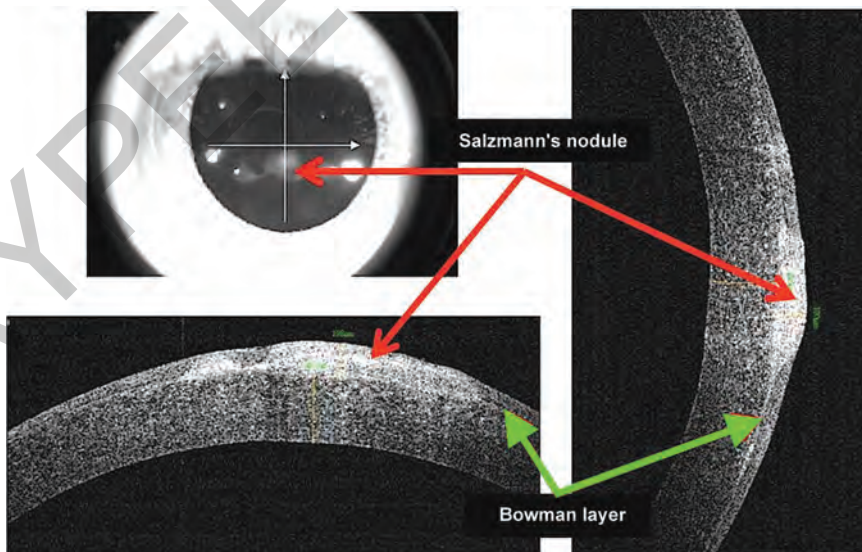


Fig. 3.12 Salzmann's nodular degeneration (SND). OCT view; the red arrows point at the nodules; the green arrows point at Bowman.

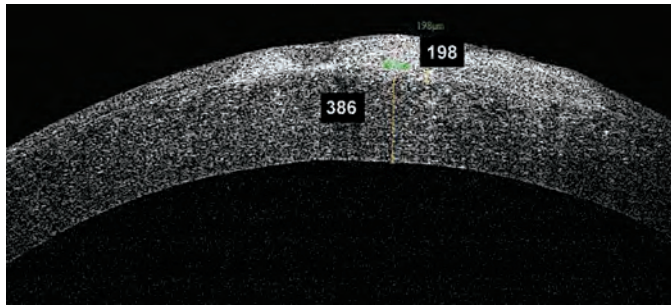


Fig. 3.13 SND. Magnified OCT view; notice the position of the nodule above Bowman layer. The lesion measures about 200 μm , while the cornea measures about 400 μm (apart from lesion).

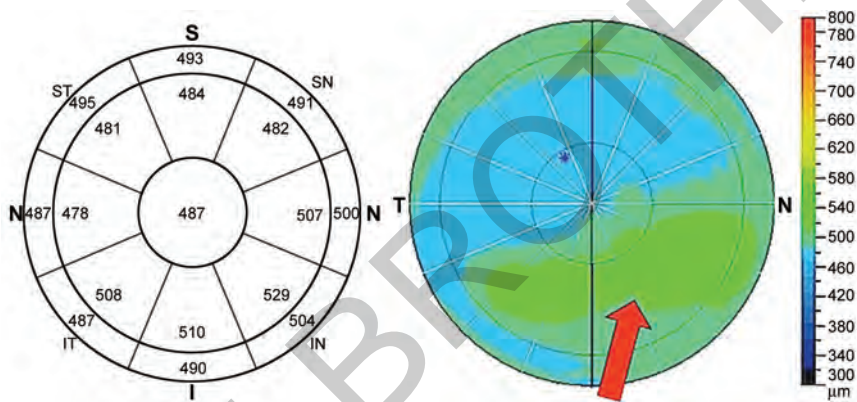


Fig. 3.14 SND. OCT pachymetry map; the red arrow points at the thick area in the map corresponding to the lesion.

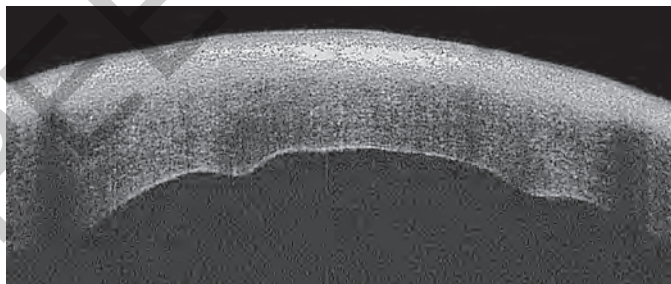


Fig. 3.15 OCT view of posterior corneal abnormality due to Descemet folds. Notice irregularity of the posterior surface.

LASIK Flap Complications

One of the major causes of induced HOAs after LASIK is related to flap cut. OCT provides a good method of measuring flap thickness and shape. Flaps created with femtosecond tend to be more uniform and regular than those created with mechanical microkeratome (MMK). **Figures 3.17 to 3.22** show the difference between MMK cut and femtosecond cut by means of central vs. peripheral and right vs. left.

Use of anterior OCT in post LASIK complications will be discussed in chapter 8.

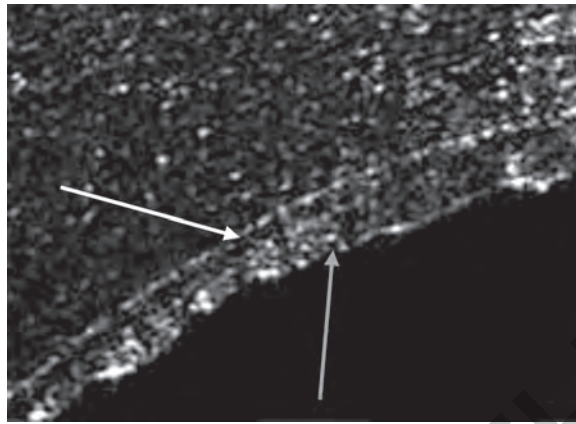


Fig. 3.16 OCT view of posterior corneal abnormality due to Fuch's endothelial dystrophy. The white arrow points at Descemet membrane and the gray arrow points at abnormal endothelial layer.

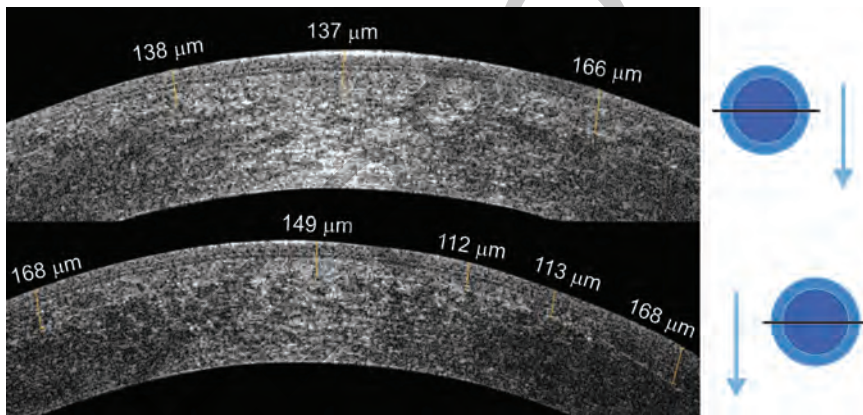


Fig. 3.17 Flap cut with MMK. A comparison between the two eyes. The upper OCT view is for the right eye and the lower is for the left. Notice the difference in thickness; the right flap is thinner than the left flap since the former was performed first.

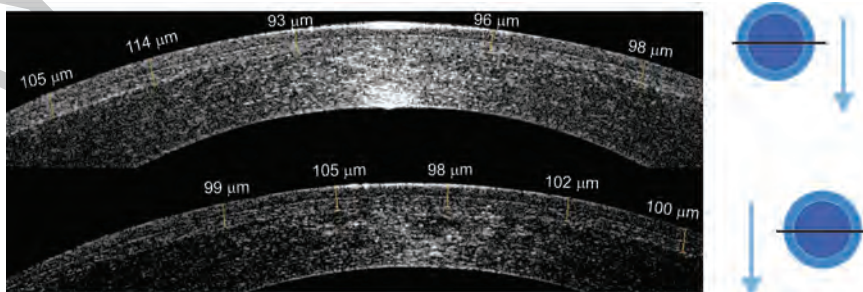


Fig. 3.18 Flap cut with femtosecond laser. A comparison between the two eyes. The upper OCT view is for the right eye and the lower is for the left. There is no significant difference in thickness.

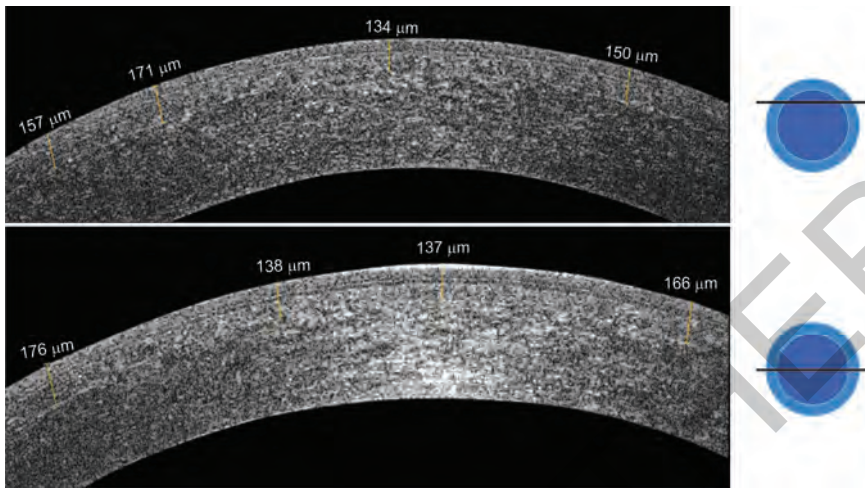


Fig. 3.19 Flap cut with MMK. A comparison between flap periphery (upper OCT view) and flap center (lower OCT view). Both views are comparable but the flap is irregular along both cuts.

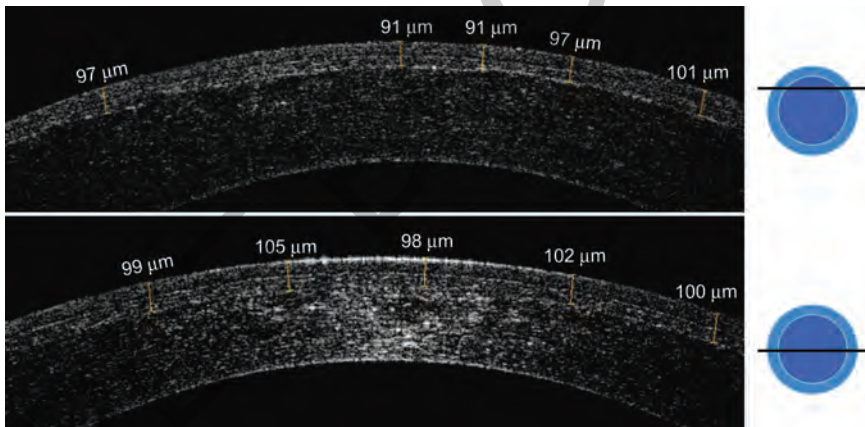


Fig. 3.20 Flap cut with femtosecond laser. A comparison between flap periphery (upper OCT view) and flap center (lower OCT view). Notice the uniform regular cut in both views and along the cuts.

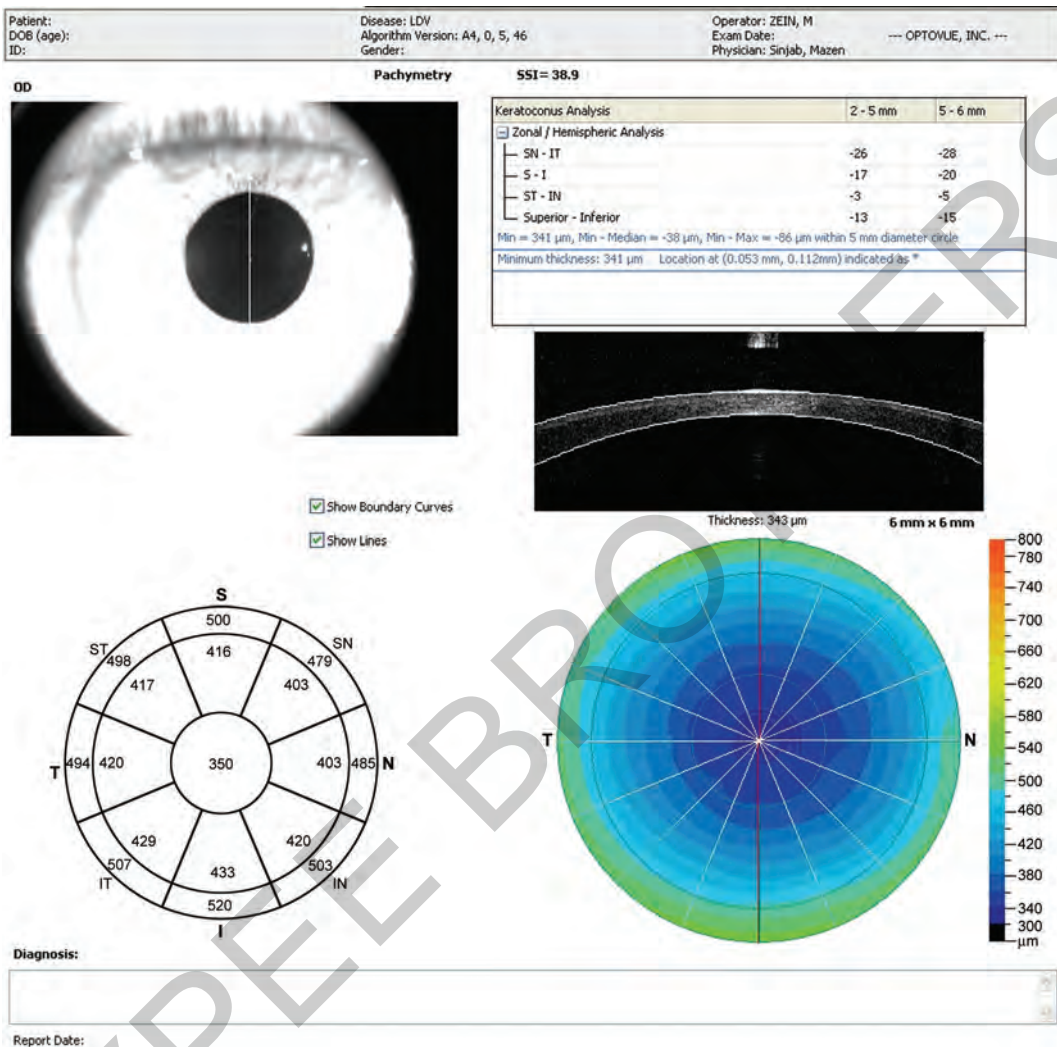


Fig. 3.21 OCT pachymetry after femtosecond flap creation in the right eye. Notice the regular concentric pattern.

